Influence of oxidation upon the CO_2 capture performance of a phenolic-resin-derived carbon

M.G. Plaza[a], K.J. Thurecht[b], C. Pevida[a], F. Rubiera[a*], J.J. Pis[a], C.E. Snape[c] and T.C. Drage[c†]

[a]*Instituto Nacional del Carbón, INCAR-CSIC, Apartado 73,33080, Oviedo, Spain.*

[b]*Australian Institute for Bioengineering and Nanotechnology and Centre for Advanced Imaging, The University of Queensland, St Lucia, Queensland, 4072, Australia.*

[c]*Department of Chemical and Environmental Engineering, Faculty of Engineering, University of Nottingham, University Park, Nottingham, UK.*

Abstract

The effect of oxidation upon the CO_2 capture performance has been studied taking a phenolic resin carbon as the base material. Oxygen surface groups were introduced through liquid and gas phase oxidation treatments, using ammonium persulfate, nitric acid and air, respectively. The surface chemistry of the final carbon is strongly affected by the type of oxidation treatment: liquid phase oxidation introduces a greater amount of oxygen, mostly as carboxylic groups; these are absent in the gas phase oxidised sample that contains mainly ether and carbonyl functionalities. The porous texture of the samples is also affected by the oxidation treatment: through liquid phase oxidation the pore volume is somewhat reduced, while this is slightly developed by air treatment at 693 K. Despite the reduction in the porous volume and the acidic surface, liquid-phase oxidised samples present greater CO_2 adsorption capacity than the starting carbon due to Lewis acid-base interactions with the CO_2 molecule. Moreover: oxidised samples are easily regenerated, and observed heats of adsorption are

† Corresponding Author: Tel : +34 985 119090; E-mail address: frubiera@incar.csic.es. (F. Rubiera)

typical from physisorption processes, which will facilitate the adsorbent regeneration in cyclic adsorption processes. Oxidation is therefore proposed as a plausible modification technique for developing easy-to-regenerate carbon adsorbents with enhanced CO_2 capture performance.

Keywords *Adsorption; oxidation; carbon materials; CO_2 capture*

1. Introduction

Carbon Capture and Storage (CCS) is expected to be a key contributor to achieve the required emissions reduction in the next decades [1]. Postcombustion CO_2 capture (PCC) consists on the separation of CO_2 from the flue gas produced by fuel combustion. As an end-of-pipe technology, it presents potential for decarbonising the energy and industrial sectors in the short term [2]. The main challenges of this technology when applied to the power sector are the vast flow rate of the flue gases, which are at near atmospheric pressure, and the low concentration of CO_2 (typically 3-15% by volume). *A priori*, this separation could be accomplished by amine scrubbing, which has been used to separate CO_2 from natural gas and hydrogen since 1930. However, there are no full-scale postcombustion capture units installed yet, due to the magnitude of the problem and the high energy penalty of the amine process. Adsorption processes present scope for reducing the energy penalty of the capture step [3, 4]. A number of different processes and cycle configurations are under study. Adsorption processes differ mainly by the regeneration method used. A first group of processes (known as temperature swing adsorption, TSA) regenerates the sorbent by increasing the temperature of the adsorber. This can be accomplished by direct heating using steam or hot CO_2 [4], by indirect heating through internal heat exchangers [5], or by means of the Joule effect, which is usually referred to as electrical swing adsorption (ESA) [6, 7]. A second group of processes regenerates the adsorbent by decreasing the system pressure. These are known as pressure swing adsorption (PSA) or vacuum swing adsorption (VSA), when the evacuation pressure is

below atmospheric pressure such as the PCC case [3, 8-10]. Finally, the regeneration method can consist in a combination of heating and evacuation [11-13]. The design of an optimised adsorption process is intrinsically related to the adsorbent properties. Therefore an important research effort has also been directed towards materials development [14-17]. The ideal adsorbent for PCC should present high stability, sufficient adsorption capacity at low CO_2 partial pressures, high selectivity, easy regeneration, and low cost. Carbon materials fulfil previous requirements, resulting appealing adsorbents for postcombustion CO_2 capture [4, 12, 18, 19].

Activated carbons are widely used in a large number of industrial applications. Their adsorption capacity is primarily determined by their porous structure but is strongly influenced by their surface chemistry. These properties can be tailored to enhance adsorption performance towards a specific adsorbate; i.e., hydrophobic activated carbons are oxidised to increase their hydrophilic character for liquid phase adsorption applications, or for their implementation in PSA driers [20]. It is well established that the electron-deficient carbon atom of CO_2 can act as a Lewis acid and participate in stabilizing reactions with Lewis base groups such as amines [21]. As a result, research has focussed on the incorporation of nitrogen functionalities onto the surface of activated carbons to promote their performance as adsorbents in CO_2 capture applications [22-26]. However, nitrogen functionalities are not the only species capable of acting as Lewis bases. Oxygen functional groups, such as carbonyls, alcohols and ethers, contain an electron-donating oxygen atom that can also participate in electrostatic interactions with CO_2 [27-29]. It is thus expected that the presence of oxygen functional groups on the carbon surface will enhance CO_2 adsorption capacity and selectivity. There is extensive literature on oxidative treatments of carbons [30-32]. However, little has been published about the influence of these treatments on CO_2 adsorption, which has been explored thoroughly for many other compounds. It is known that the interaction between

carbonyls and CO_2 involves greater electron transfer than that of benzene and CO_2 [33]; therefore these groups are expected to be stronger adsorption sites than the delocalised π electrons arising from the micrographites that constitute the carbon. Deitz and co-workers differentiated long ago three levels of interaction of CO_2 with carbons: pure physisorption (present in carbon black), formation of bicarbonate type adsorption complexes with surface hydroxyl groups, and formation of stronger complexes with carbonate structure [27]. Carboxylic acids have also shown to present strong Lewis acid-Lewis base interactions with the CO_2 molecule: they present a carbonyl group that can act as a Lewis base towards the carbon atom (Lewis acid) of the CO_2 molecule, but also an acidic proton that can act as a Lewis acid towards the oxygen atoms (Lewis bases) of the CO_2 molecule [28, 34]. An experimental study carried out with functionalised microporous organic polymer networks has recently pointed out that the carboxylic acid functionalised network shows higher isosteric heat of adsorption than its amine analogue [35]. Molecular simulation results indicate that the density of the adsorbed CO_2 is increased by *ca.* 56% in carboxyl functionalised slit pores [29].

In this work oxygen surface functionalities were introduced by a number of different techniques onto the surface of an activated carbon with the aim of studying their influence over the CO_2 capture performance of the oxidised materials. The degree of surface oxidation, the nature of the resulting surface oxides, and the adsorption properties of the oxidised carbons depend on the nature of the starting material, the oxidising agent used, the temperature of the reaction, and the length of the treatment. Gas phase oxidation increases mainly the concentration of hydroxyl and carbonyl surface groups, while oxidation in the liquid phase increases primarily the concentration of carboxylic acids [36]. The total amount of oxygen incorporated through the different oxidation treatments was determined by ultimate analysis, and the nature of the surface oxides formed was elucidated by means of

temperature programmed desorption tests (TPD) and X-ray photoelectron spectroscopy (XPS). It must be noted that the oxidation of an activated carbon may also change its physical structure: in the case of oxidation in the liquid phase, the major reaction is the formation of surface functional groups, although some gasification may also take place depending upon the strength of the oxidative treatment and the severity of the experimental conditions. For gas phase oxidations, the reaction of oxygen with the carbon below 673 K predominantly results in the formation of carbon-oxygen surface functional groups, whereas above 673 K the decomposition of surface compounds and the gasification of the carbon are the predominant reactions [37]. To account for these effects, the texture of oxidised carbons was characterised by N_2 adsorption at 77K.

2. Experimental

2.1. Oxidation of activated carbons

Oxidised carbons were produced by modifying a spherical phenolic-resin-derived activated carbon supplied by MAST Carbon Ltd. [38], from now on referred as M. This was used as the base material for which different oxidation treatments were compared.

A first series of oxidised carbons were prepared by stirring 1 g of carbon in 10 cm^3 of a saturated solution of ammonium persulfate in sulphuric acid 1 M at room temperature for different periods of time: 1, 3 and 24 h [30]. The samples will be referred as MAP-1, MAP-3 and MAP-24, respectively. The excess solution was removed by repeated washing of the treated carbon with water purified by reverse osmosis (Milli-RO), until the washings presented neutral pH. Finally the samples were dried overnight in a vacuum oven at 373 K and 150 mbar.

A series of nitric acid oxidised carbons were prepared by placing 1 g of carbon in a round bottom flask with 10 cm^3 nitric acid (1 M and 16 M). The contents were stirred at 363 K for different periods of time: 1, 3 and 24 h. All the samples were thoroughly washed with

purified water until the washings were no longer acidic. Finally, the samples were dried overnight in a vacuum oven at 373 K and 150 mbar. The carbons produced by this treatment will be referred as MNA1-1, MNA1-24, MNA16-1 and MNA16-3. It is expected that the extent of oxidation will increase at the higher concentration of nitric acid. It has been previously reported that temperatures in the range of 353-373 K are required to provide an adequate rate of oxidation [20].

A gas phase oxidised carbon was prepared by heating 1 g of carbon in a horizontal furnace under a flow rate of 100 cm^3 min^{-1} of nitrogen, until the desired temperature (693 K) was reached. Following, a flow rate of 10 cm^3 min^{-1} of dry compressed air was added to the nitrogen stream, and the sample was held at this temperature for additional 3 h, before being cooled to room temperature under nitrogen. The carbon obtained was denoted as MAM. The temperature of 693 K was selected because it has been reported to be the optimum temperature for the formation of surface oxides [39, 40]. Prior to oxidation the reactivity profile in air of the raw carbon was obtained in a thermobalance TA Q500.

2.2. Chemical and textural characterisation of oxidised samples

The textural characterisation of the samples was carried out by obtaining the N_2 adsorption isotherms at 77 K in a Micromeritics TriStar® 3000. Samples were outgassed at 373 K under vacuum for 24 h prior to adsorption measurements. The total pore volume (V_p) was evaluated by the total amount of adsorbed nitrogen at a relative pressure of 0.99, and the micropore volume (V_{DR}) was calculated by the Dubinin-Radushkevich equation. The apparent surface area of the samples was estimated through the BET equation [41] (S_{BET}) in the relative pressure range between 0.02 and 0.08.

The extent of the oxygen incorporation through the different oxidation treatments was determined by the ultimate analysis of the samples. The acid nature of the oxygen functionalities introduced was assessed by means of the Point of Zero Charge (pH_{PZC}), as it

gives an idea of the ratio of basic to acid surface groups. The pH_{PZC} was estimated by means of a mass titration method adapted from Noh and Schwarz [42]. This entailed preparing a suspension of 100 mg of each sample in 0.5 cm^3 purified water, shaking it under an inert atmosphere for 24 h and then measuring the pH of the suspension. This protocol was repeated by adding subsequent aliquots of 0.1 cm^3 of purified water to obtain a progressively less concentrated suspension. The value of pH_{PZC} was estimated from the average pH of the suspensions containing between 12 and 8 wt.% of solid, a range in which the pH was approximately constant.

Temperature programmed desorption (TPD) tests were carried out in a thermobalance SETARAM TGA92 coupled to a MS spectrometer (OmniStar, Balzers Instruments) through a heated interface. These tests entailed heating the samples up to 1273 K in 50 cm^3 min^{-1} of Ar at a heating rate of 15 K min^{-1}. The amount of evolved CO and CO_2 was semi quantitatively determined using calcium oxalate as a standard.

Characterisation of the surface chemistry of the adsorbent was completed by X-ray photoelectron spectroscopy (XPS) on a Kratos AXIS ULTRA with a mono-chromated A1Kα X-ray source (energy 1486.6 eV) operated at 15 mA emission current and 10 kV anode potential. The ULTRA was used in FAT (fixed analyser transmission) mode, with pass energy of 20 eV for high resolution scans. The magnetic immersion lens system allows the area of analysis to be defined by apertures. A 'slot' aperture of 300 x 700 μm for wide/survey scans and high resolution scans was used. The high resolution scans were charge corrected to the main C1s peak at 284.8 eV. Elemental quantification was corrected using a standard of indium wire and was used to characterise different forms for carbon and oxygen.

2.3. CO_2 adsorption studies

The partial pressure of CO_2 in flue gas is usually below 0.2 bar, so it is important to study the equilibrium of adsorption of CO_2 at subatmospheric pressures. Equilibrium measurements

were carried out at 273 K in the pressure range between 0.002 and 1.2 bar using an automatic apparatus TriStar® 3000 from Micromeritics (accuracy within 0.5%). Samples were previously outgassed at 373 K under vacuum for 24 h.

The dynamic CO_2 capture performance of the samples was evaluated at atmospheric pressure in a thermogravimetric analyser TA Q500. Prior to the adsorption measurements, the samples were dried at 383 K in 100 cm^3 min^{-1} of He for 30 min, and then allowed to cool to 298 K. Helium was selected as purge gas because it presents negligible adsorption at room temperature. The CO_2 adsorption capacity at 298 K was assessed by the mass gain experienced by *ca.* 15 mg of sample when the flow rate was changed to 74 cm^3 min^{-1} of pure CO_2. After 30 min the flow was changed again to He to study the regeneration of the samples. The capture capacity will be given in terms of mmol of adsorbed CO_2 per g of dry adsorbent. The heat of adsorption was evaluated by means of a calorimeter TA DSC Q 2000, following the same procedure as for the isothermal adsorption/desorption tests described before, and using indium for calibration purposes.

A series of non-isothermal CO_2 capture tests were also carried out in the thermogravimetric analyser to study the influence of temperature upon the adsorption capacity of the samples [43]. The tests were similar to the isothermal experiments, but at the end of the CO_2 capture step at 298 K, instead of changing the feed gas to He, the temperature was raised to 383 K at a heating rate of 0.25 K min^{-1} in CO_2 flow. This heating rate was considered to be sufficiently slow as to allow near equilibrium conditions.

3. Results and discussion

3.1. Properties of the original carbon, M

M is essentially a microporous carbon with a BET surface area of 1180 m^2 g^{-1} (textural characterisation is summarised in Table 1). In its unaltered state the material is predominantly composed of carbon (97.8%) with minor O, H, and N (Table 2). Figure 1 represents the mass

loss profile of the raw material, M, obtained in a thermobalance TA Q500, during heating in a stream containing 40 cm^3 min^{-1} of nitrogen (purge gas) and 50 cm^3 min^{-1} of air (sample gas) at a heating rate of 5 K min^{-1}. As can be seen from the profile of mass loss, the carbon contains negligible ash content, as expected for a resin-derived activated carbon. Two main stages can be clearly differentiated in the curves: the first between 700 and 940 K and the second from 940 to 1100 K. This can be explained by the presence of two types of carbon in the raw sample that present different reactivity towards oxygen, as proposed in previous studies from other authors [38].

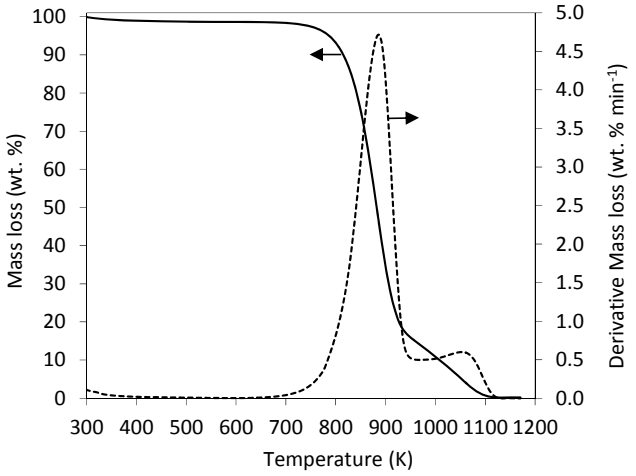

Figure 1. Combustion profile of M in 40 cm^3 min^{-1} of N_2 (purge gas) and 50 cm^3 min^{-1} of air (sample gas) at a heating rate of 5 K min^{-1}.

3.2. Chemical and Textural Properties

Table 1 summarises the textural parameters of the studied samples and illustrates the effect of the oxidation techniques on the textural properties compared to the original carbon, M. The carbons are essentially microporous (micropore volume represents nearly 90% of total pore volume). Liquid phase oxidation treatments (MAP and MNA series) decreased the micropore volume of the carbons by similar amounts (20% on average). This reduction is mainly due to the presence of embedded functional groups [44], although it can be partly attributed to a

partial collapse of pore walls caused by the oxidation reaction and the surface tension of the oxidising solution [45]. On the other hand, the gas phase oxidised sample presents a slightly higher pore volume and BET surface area than the starting carbon. This moderate texture development is due to the partial gasification of the carbon with air.

Table 1 Textural parameters and helium densities of the studied samples

Sample	d_{He} ($g\,cm^{-3}$)	N_2 adsorption, 77 K		
		S_{BET} ($m^2\,g^{-1}$)	V_{DR} ($cm^3\,g^{-1}$)	V_p ($cm^3\,g^{-1}$)
M	1.99	1180	0.44	0.51
MAP-1	1.99	928	0.35	0.39
MAP-3	1.93	929	0.35	0.42
MAP-24	1.96	887	0.34	0.38
MNA1-1	1.99	894	0.34	0.38
MNA1-24	1.96	917	0.35	0.39
MNA16-1	1.96	941	0.36	0.41
MNA16-3	1.96	962	0.36	0.41
MAM	2.02	1196	0.46	0.53

The ultimate analysis of the oxidised samples is presented in Table 2. The elemental composition is given in wt.%, dry ash free basis (daf). From the table it can be seen that all the oxidation treatments successfully introduced a significant amount of oxygen into the carbons. The amount of oxygen introduced is dependent upon the oxidation agent and also on the length of the treatment. The adsorbents prepared with concentrated nitric acid, MNA16 series, yielded the highest oxygen content, up to 15.9 wt.%, and the sample oxidised with air, MAM, the lowest: 5.4 wt.%. Stronger acid solutions and longer oxidation times lead to the formation of higher amounts of surface oxygen complexes. All these findings are in good agreement with the literature [46]. A small increase in the nitrogen content of the nitric acid-treated samples was observed, from 0.28 up to 0.77 wt.%, probably due to the formation of nitro and nitrate groups, as it has been discussed elsewhere [47]. Further analysis to determine the composition and type of oxygen functional groups introduced to the surface

was made by TPD and XPS analysis and will be discussed in context of the CO_2 adsorption performance of the carbons.

Table 2 Ultimate analysis of the samples

Sample	Ultimate analysis (wt.%, daf)[a]				
	C	H	N	S	O
M	97.78	0.46	0.28	0.07	1.41
MAP-1	91.32	1.18	0.31	0.20	6.99
MAP-3	89.85	1.26	0.30	0.17	8.42
MAP-24	86.54	1.41	0.28	0.25	11.52
MNA1-1	90.21	1.06	0.77	0.15	7.81
MNA1-24	86.49	1.22	0.77	0.15	11.37
MNA16-1	82.69	1.75	0.77	0.23	14.56
MNA16-3	80.63	2.37	0.77	0.33	15.90
MAM	92.62	1.31	0.49	0.15	5.43

[a] **Per cent in weight,** dry ash free basis

3.3. CO_2 adsorption capacity: influence of textural properties and surface chemistry.

The equilibrium adsorption capacity of CO_2 at 273 K and 0.1 bar of the oxidised samples is presented in Table 3. Although the absolute differences might not seem high, liquid phase oxidised samples tend to present higher adsorption capacities than the parent carbon (up to +17%, in the case of MNA16-3). Sample MAM, which showed the highest pore volume of the oxidised series (and the lowest oxygen content), is the sole sample which capacity is slightly below that of the parent carbon.

Table 3 Equilibrium adsorption capacity of CO_2 at 273 K and 0.1 bar

Sample	CO_2 adsorbed at 0.1 bar and 273K (mmol g^{-1})
M	1.04
MAP-1	1.04
MAP-3	1.05
MAP-24	1.13
MNA1-1	1.12
MNA1-24	1.18
MNA16-1	1.18
MNA16-3	1.22
MAM	0.96

The CO_2 adsorption capacity at 298 K and atmospheric pressure, obtained by means of the dynamic CO_2 adsorption/desorption tests carried out in the thermogravimetric analyser, is summarised in Table 4 (at least two repetitions carried out; standard deviation shown). Liquid phase oxidised samples also present higher CO_2 adsorption capacity than the starting material, M, at room temperature and atmospheric pressure (up to +26% in the case of MAP-3). Obtained CO_2 capture capacities, up to 2.9 mmol CO_2 g^{-1} at 298 K, are higher than the capacity of commercial activated carbons evaluated under similar conditions (between 1.6 and 2.1 mmol CO_2 g^{-1}) [23, 48]. The comparison is still positive when compared with other surface modifications, such as nitrogen enrichment: modification of an activated carbon with ammonia resulted in materials with CO_2 capacities up to 2.2 mmol CO_2 g^{-1} at 298 K tested under similar conditions [23]. Likewise, urea-formaldehyde, melamine-formaldehyde and phenolic resin-derived carbons have been reported to present capacities between 1.8 and 2.5 mmol CO_2 g^{-1} at 298 K [22, 49, 50].

Table 4 Dynamic CO_2 adsorption capacity at 298 K and 1 bar

Sample	CO_2 uptake (mmol CO_2 g^{-1} dry adsorbent)	Standard deviation	Number of repetitions
M	2.3	0.1	2
MAP-1	2.4	0.3	4
MAP-3	2.9	0.1	2
MAP-24	2.8	0.1	2
MNA1-1	2.6	0.1	2
MNA1-24	2.5	0.1	2
MNA16-1	2.5	0.4	2
MNA16-3	2.7	0.1	4
MAM	2.3	0.1	4

Note that higher texture development of MAM is not translated into higher adsorption capacity: the maximum CO_2 uptakes were obtained for the liquid phase oxidised samples. Thus it seems that surface chemistry is playing an important role in the adsorption of CO_2. The adsorption enhancement of the liquid phase oxidised samples compared to the parent

carbon needs to be related to stronger adsorbate-adsorbent interactions between the introduced oxygen surface groups and the CO_2 molecule. The nature of this interaction may be Lewis acid-base reactions between the carbon electron acceptor of the CO_2 molecule and the oxygen electron donors present on the surface of the oxidised carbons.

Figure 2 presents the results of the dynamic CO_2 adsorption/desorption tests carried out at 298 K in the thermogravimetric analyser; the CO_2 uptake has been divided by the capture capacity (shown in Table 4) to facilitate the comparison of the rates of the two processes. As can be seen from the figure, all the samples are easily regenerated by simply changing the feed gas from CO_2 to He at 298 K (above 95 % of all the adsorbed CO_2 was desorbed after 30 min). The calorimetric measurements showed that the specific heat of adsorption of CO_2 over the studied samples lies in the range of 48-68 kJ kg^{-1}, which is very small compared to the heat of absorption of CO_2 in MEA solutions (1864 kJ kg^{-1}) [51], commonly used in the industrial amine scrubbing process to separate CO_2 from gaseous streams. One of the major drawbacks of the application of amine scrubbing to post-combustion capture is the energy penalty associated to the solvent regeneration (the steam cost accounts for 50% of the running cost of the plant) [52]. The use of adsorbents could therefore contribute to reduce the energy penalty associated to the capture step. The specific heat of adsorption in terms of kJ per kg of adsorbent can be divided by the amount of CO_2 adsorbed per kg of adsorbent, to obtain the more common units of kJ mol^{-1} CO_2. The calculated heat of adsorption falls within 20-28 kJ mol^{-1}, values in the range of physisorption processes.

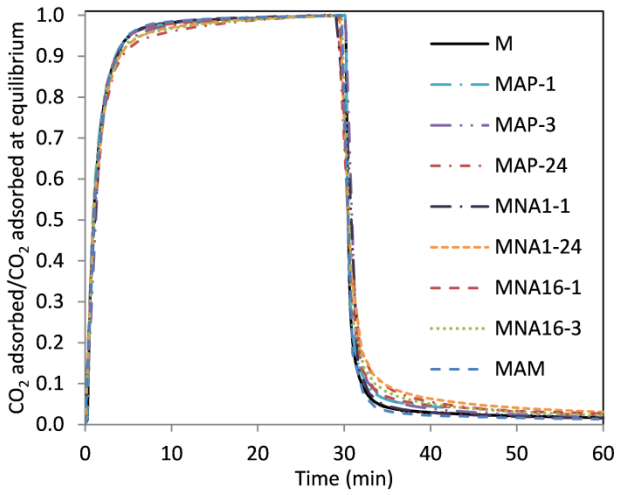

Figure 2. Dynamic CO_2 adsorption/desorption tests carried out at 298K and 1 bar; adsorption: 74 cm^3 min^{-1} of pure CO_2 flow; desorption: 100 cm^3 min^{-1} of He flow.

The amount of CO_2 adsorbed decreased gradually with increasing temperature during the non-isothermal capture tests, as expected for a physical adsorption process. The values fall from 2-3 mmol CO_2 g^{-1} at 298 K, to *ca.* 0.5 mmol CO_2 g^{-1} at 383 K. As it has been already discussed, adsorption is governed by both textural development and surface chemistry, so to assess individually the effect of the introduced oxygen surface functionalities, the CO_2 capture capacity of the samples was normalised by the micropore volume, V_{DR}, (responsible for CO_2 adsorption at atmospheric pressure) [50]. The corresponding results are shown in Figure 3. In the studied temperature range, liquid phase oxidized adsorbents present higher CO_2 adsorption capacity per cm^3 of micropore volume than M (increased packing density). These results are in good agreement with recently published molecular simulation studies [44].

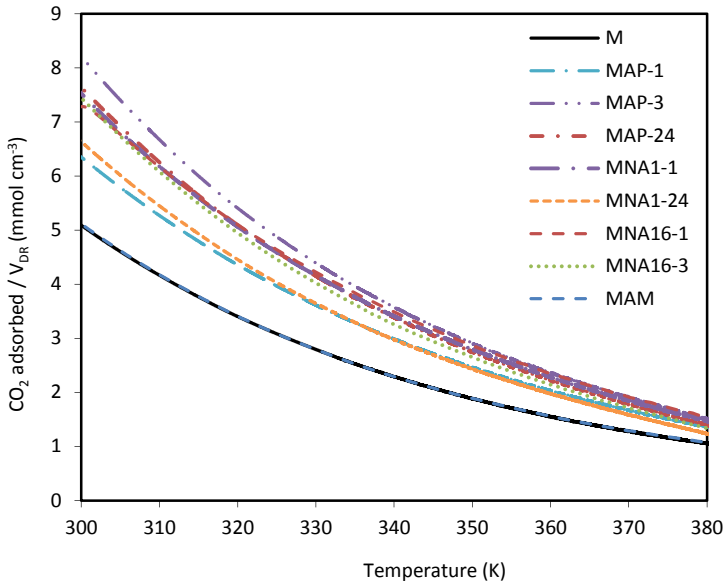

Figure 3. Non-isothermal CO_2 capture tests carried out in 74 cm^3 min^{-1} of CO_2 flow (heating rate of 0.25 K min^{-1}).

The acid-base character of the carbons' surface was probed by measuring the point of zero charge (Table 5). The starting carbon, M is basic as expected from its low oxygen content. The drop in the pH_{PZC} observed for the oxidised samples clearly shows that the oxygen introduced onto these carbons is mostly acid in nature. Liquid phase oxidised samples presented a sharp and relatively similar reduction in pH_{PZC}, whereas the gas phase oxidised sample presented a lesser decrease in pH_{PZC}. Note that the samples with the lowest pH_{PZC} present the highest CO_2 uptake at 298 K. This is remarkable because to date focus was made in introducing basic moieties to enhance the adsorption of acidic CO_2. The increment in acidity due to the nitric acid treatment is controlled by the concentration of the solution and the contact time with the carbon. In general, extended oxidation times lead to a further decrease in the pH_{PZC}. The carbon with the lowest pH_{PZC} is MAP-24 (Table 5), yet this sample does not have the highest oxygen content. This is in good agreement with previous experimental results from other authors [47]. As the value of pH_{PZC} indicates the ratio of basic to acid surface groups, it seems that the different oxidising agents are introducing

different types (or different relative amounts) of oxygen groups, with varying acidic character. Carboxyls, lactones and phenols are associated with the acidic behaviour of carbon surfaces, whereas ethers, carbonyls, quinones and pyrones, are responsible for their basic properties [53].

Table 5 Point of Zero Charge (pH_{PZC}) of the samples

Sample	pH_{PZC}
M	8.5
MAP-1	3.3
MAP-3	2.6
MAP-24	2.2
MNA1-1	3.3
MNA1-24	2.9
MNA16-1	3.0
MNA16-3	2.7
MAM	5.3

To quantify the nature of the oxygen groups introduced and their relative amounts, TPD tests and XPS analysis of the oxidized samples were performed. The TPD technique relies on the heating of a carbon in an inert atmosphere, during which the oxygen surface complexes of a carbonaceous material decompose releasing CO_2 and CO. The decomposition of carboxyls and lactones releases CO_2, while phenols, carbonyls, quinones and pyrones release CO, and anhydrides release simultaneously CO_2 and CO [36, 47, 54, 55]. Table 6 compiles the total amount of CO and CO_2 evolved during the TPD tests. As can be seen from the table, the oxidising treatments increase the amount of evolved CO and CO_2. Sample MNA16-3 released the greatest amount of CO and CO_2 and M the lowest, which correlated with their respective oxygen content (Table 2). The two gases are evolved in different proportions, with the ratio of CO/CO_2 reduced for the liquid phase oxidised samples compared to the starting material. The opposite trend in this ratio, an increase compared to the original carbon, is observed for the sample oxidised with air (MAM). It should be noted that this carbon gave

the highest pH_{PZC} among the oxidised samples. The CO and CO_2 desorption profiles are depicted in Figure 4 for samples M, MAP-24, MNA16-3 and MAM; similar desorption profiles were obtained for the other oxidised samples. The influence of the oxidising agent and the resultant surface oxygen functional groups can be observed from the different shapes of the profiles.

Table 6 Amount of CO and CO_2 evolved during heating up to 1273 K in Ar flow

Sample	CO_2 ($mmol \cdot g^{-1}$)	CO ($mmol \cdot g^{-1}$)	CO/CO_2
M	0.15	0.56	3.6
MAP-1	0.72	1.81	2.5
MAP-3	0.75	1.66	2.2
MAP-24	1.55	3.24	2.1
MNA1-1	0.88	1.87	2.1
MNA1-24	1.15	2.08	1.8
MNA16-1	1.84	2.15	1.2
MNA16-3	2.04	4.25	2.1
MAM	0.35	2.72	7.7

MNA16-3 sample evolves CO_2 at a maximum rate at 570 K with a shoulder around 700 K and a smaller shoulder around 940 K that tails up to 1273 K. In the case of MAP-24, the maximum rate of CO_2 evolution is shifted to lower temperatures, 523 K; it plateaus out between 600 and 750 K with a shoulder around 950 K, and peaks again slightly at 1240 K. A smaller amount of CO_2 is also evolved from these samples at low temperatures, between 300 and 400 K. The CO_2 emissions profile from MAM differs significantly from the solution modified carbons, starting above 400 K with minor contributions below 760 K. The temperature of maximum CO_2 evolution is shifted to higher temperatures, approximately 950 K. Finally, M evolves CO_2 at a maximum rate *ca.* 1000 K. The low temperature emissions detected for the liquid phase oxidised samples may come from desorbed CO_2, and not from the decomposition of a surface oxide. The CO_2 emission between 400 and 600 K mainly observed for samples MAP-24 and MNA16-3 can be undoubtedly attributed to the

decomposition of carboxylic groups [36, 54, 56, 57]. It is important to note that this peak is of significant greater intensity in the liquid phase oxidised samples. The CO_2 evolved at higher temperatures may be related to the decomposition of carboxylic anhydrides and lactones, that decompose in the range 600 to 950 K [36, 54, 56, 57]. There is little information regarding the assignment of higher temperature CO_2; to some extent, it might come from secondary reactions of CO.

The CO profiles show that MNA16-3 releases CO at the maximum rate at 1000 K, with shoulders above 700 K and at 1160 K, and a small peak at 550 K. The CO profile for MAP-24 presents a small peak at 500 K, and the maximum rate of CO evolution at around 1160 K with a shoulder above 700 K and a plateau from 950 K. MAM only evolves CO at high temperature with a maximum at 1000 K and a shoulder at 1160 K. M starts releasing a small amount of CO from 460 K, but reaches the maximum rate at 1250 K. CO desorption at relatively low temperatures (below 600 K) may come from the decomposition of aldehydes or ketones, whereas at higher temperatures, above 600 K can be assigned to the decomposition of more stable carboxylic anydrides (see the simultaneous evolution of CO_2) [54]. Desorption of CO around 900 K is likely associated to the decomposition of phenolic groups, whereas at around 1000 K this might be related to the decomposition of ethers, carbonyls and quinones [36]. Higher temperature evolution of CO, at around 1200 K, has been associated to the decomposition of pyrone groups [54]. The presence of such groups on the surface of M, together with delocalised π electrons, may account for its basic character [58]. In general, the CO_2 and CO profiles of samples MAP-24 and MNA16-3 yield the same individual contributions, although with different relative abundance; this may explain the lower value of pH_{PZC} of MAP-24 when compared to MNA16-3 which has a higher total oxygen and evolved CO_2.

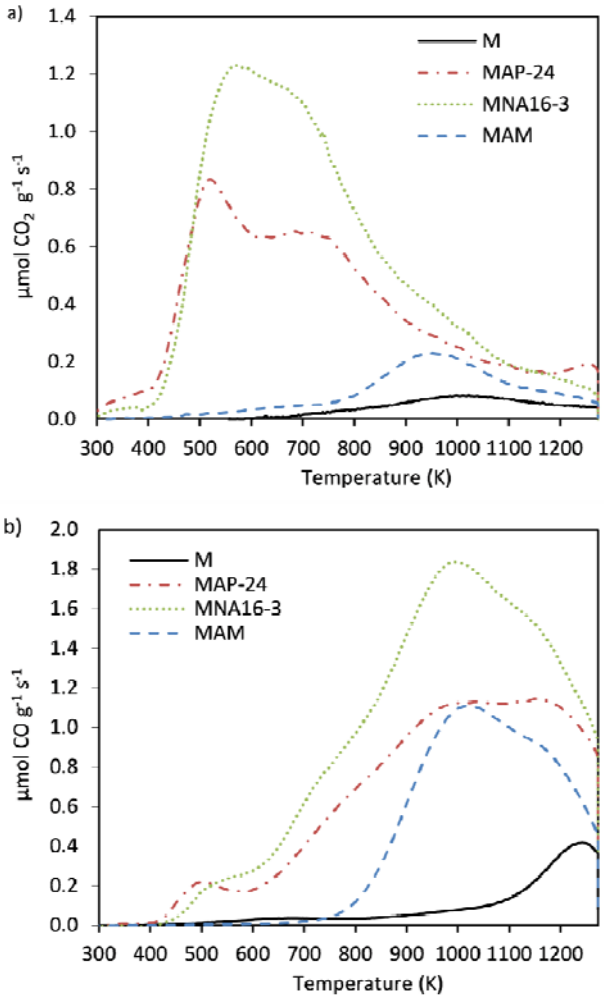

Figure 4. Temperature Programmed Desorption (TPD) tests with evolved gas analysis by MS of samples M, MAP-24, MNA16-3 and MAM: CO_2 (a) and CO (b) evolution profiles during heating in 50 cm^3 min^{-1} of Ar flow at a heating rate of 15 K min^{-1}.

XPS analysis was performed on 4 carbons (MAP-24, MNA1-1, MNA16-3 and MAM) to further study the nature of the surface oxygen groups formed upon oxidation. The wide scans confirm that the surface is composed mainly of carbon and oxygen, with the amount of oxygen dependent upon the oxidation treatment applied (Table 7). In agreement with the ultimate analysis of the bulk sample (Table 2), the solution state oxidised MNA16-3 gives the highest oxygen concentration, whilst air modification (MAM) provides the lowest. Overall there is a good agreement between the proportion of bulk and surface oxygen determined by

ultimate and XPS analysis, respectively. High resolution scans were performed on the C1s and O1s to identify the carbon and oxygen species present, the assignment and molar abundance of which are summarised in Table 7. A complicated envelope was produced for the C1s, and was deconvoluted into six components commonly assigned in the analysis of carbon materials to: (a) carbide, (b) graphitic carbon, (c) aliphatics, (d) hydroxyls/ethers, (d) carbonyls, and (f) carboxyls/esters [59-64]. The O1s spectra is less complicated, with only 2 components fitted (Table 7), assigned to: (a) C=O in carbonyl and carboxyl groups, and (b) singly bonded oxygen assigned to -O- or C-OH in hydroxyl and carboxylic functional groups [60, 64]. A similar proportion of each of the assigned carbon types is observed for the four carbons analysed, with graphitic carbon the dominant component present. The functional groups present on the surface of the modified carbons support the assignments of functional groups determined by the TPD analysis, with phenol, carbonyl, and carboxyl/esters groups identified. The XPS analysis presents some limitations that can be compensated with complementary information: for example, the C1s spectral peak at 288.2 eV (f) can be assigned to carboxyl or ester type functional groups, the relative proportion of which cannot be resolved by XPS. Similarly, the O1s peak at 531.3 eV (a) can be assigned to carbonyls or carboxyls. However, evidence from the TPD analysis suggests that there is little or no carboxylic functionality in the MAM sample, so these peaks must correspond to esters and carbonyls, respectively. These groups may be forming part of lactones, anhydrides, quinones or pyrones, as proposed from the analysis of the TPD.

Table 7. Deconvolution results of the XPS spectra for the modified carbons and assignments

Region	Peak	Position (eV)	Intensity (mol%) MAP-24	MNA1-1	MNA16-3	MAM	Assignment
C1s	a	283.5 ± 0.1	3.9	3.5	2.7	4.9	Carbide
	b	284.3 ± 0.1	60.6	61.8	58.9	63.4	Graphite
	c	285.0 ± 0.1	12.2	11.9	11.7	11.8	Aliphatics
	d	285.8 ± 0.1	6.4	6.6	7.1	6.7	C-OH and C-O-C
	e	286.6 ± 0.2	3.6	3.8	3.1	3.9	C=O
	f	288.2 ± 0.3	1.4	1.6	2.1	1.4	COOH and C(O)-O-C
	Total		88.1	89.1	85.5	92.1	
O1s	a	531.3 ± 0.1	4.8	4.4	6.7	3.0	=O in carbonyl /carboxyl
	b	532.9 ± 0.1	7.1	6.5	7.7	4.9	-O- and C-OH in carboxyl /hydroxyl
	Total		11.9	10.9	14.4	7.9	

It can be concluded that oxidation with nitric acid and ammonium persulfate introduces similar types of surface oxides, although in different relative proportions. According to the temperature assignments found in the literature [36], these groups are carboxylic acids, carboxylic anhydrides, lactones, phenols, carbonyls and quinones. On the other hand, the gas treated sample does not contain carboxyls, but it does present a combination of the thermally more stable lactones, phenols, carbonyls and ethers. The starting carbon presents mainly pyrone-like functionalities with smaller contributions of least stable species.

Therefore carboxylic acids, present in the liquid phase oxidised samples, but not in the air oxidised sample or the starting carbon, probed to favour CO_2 adsorption, which is in good agreement with recent molecular simulation studies [29, 44].

4. Conclusions

The oxidising treatments increased drastically the oxygen content of the starting carbon from 1.41 up to 15.90 wt.%. Liquid phase oxidation yields higher oxygen contents (and more

acidic surfaces) than gas phase oxidation with air. Oxidation with concentrated nitric acid introduced the highest amount of oxygen in the samples, while ammonium persulfate oxidation produced the sample with the most acidic surface. The results from TPD-MS tests indicate that liquid phase oxidation leads to the formation of carboxyls, anhydrides, lactones, phenols, quinones and pyrones, whereas air oxidation mainly leads to the formation of lactones, phenols, quinones and pyrones. Oxidation in the liquid phase decreases the pore volume and the BET surface area of the samples, whereas oxidation with air increases them slightly.

The oxygen functionalities introduced through liquid phase oxidation promote CO_2 adsorption (up to +26 % of the parent carbon at 298 K and 1 bar) in spite of their predominant acidic nature. Carboxylic acids, present in liquid-phase oxidised samples, present strong Lewis acid-Lewis base interactions with the CO_2 molecule. Thus, oxidation might be a possible modification pathway for increasing the affinity of an activated carbon towards CO_2 adsorption. Moreover, the samples are easily regenerated, with heats of adsorption typical of physisorption processes, thus offering a promising option for reducing the costs associated to the capture step in the implementation of CO_2 Capture and Storage processes.

Acknowledgements

The authors would like to thank MAST Carbon International for supplying the carbon material for further modification. TD and CS acknowledge Engineering and Physical Science Research Council for funding (EP/G063176/1). MGP acknowledges the support received from the CSIC I3P program co-financed by the European Social Fund.

References

[1] IEA. Energy Technology Perspectives 2010. Paris: International Energy Agency; 2010.

[2] IPCC, *IPCC special report on carbon dioxide capture and storage*. 2005, IPCC: Cambridge, United Kingdom and New York, NY, USA. p. 442.

[3] Ho MT, Allinson GW, Wiley DE. Reducing the cost of CO_2 capture from flue gases using pressure swing adsorption. Ind. Eng. Chem. Res. 2008;47:4883-90.

[4] Radosz M, Hu X, Krutkramelis K, Shen Y. Flue-gas carbon capture on carbonaceous sorbents: toward a low-cost multifunctional carbon filter for "green" energy producers. Ind. Eng. Chem. Res. 2008;47:3783-94.

[5] Merel J, Clausse M, Meunier F. Experimental investigation on CO_2 post-combustion capture by indirect thermal swing adsorption using 13X and 5A zeolites. Ind. Eng. Chem. Res. 2008;47:209-15.

[6] Grande CA, Ribeiro RPPL, Rodrigues AE. CO_2 capture from NGCC power stations using electric swing adsorption (ESA). Energy & Fuels 2009;23:2797–803.

[7] Grande CA, Rodrigues AE. Electric swing adsorption for CO_2 removal from flue gases. Int. J. Greenh. Gas Control 2008;2:194-202.

[8] Zhang J, Webley PA, Xiao P. Effect of process parameters on power requirements of vacuum swing adsorption technology for CO_2 capture from flue gas. Energ. Convers. Manage. 2008;49:346-56.

[9] Delgado JA, Uguina MA, Sotelo JL, Águeda VI, Sanz A, Gómez P. Numerical analysis of CO2 concentration and recovery from flue gas by a novel vacuum swing adsorption cycle. Computers & Chemical Engineering 2011;35:1010-9.

[10] Xu D, Zhang J, Li G, Xiao P, Webley P, Zhai Y-c. Effect of water vapor from power station flue gas on CO2 capture by vacuum swing adsorption with activated carbon. Journal of Fuel Chemistry and Technology 2011;39:169-74.

[11] Ishibashi M, Ota H, Akutsu N, Umeda S, Tajika M, Izumi J, Yasutake A, Kabata T, Kageyama Y. Technology for removing carbon dioxide from power plant flue gas by the physical adsorption method. Energ. Convers. Manage. 1996;37:929-33.

[12] Dutcher B, Adidharma H, Radosz M. Carbon filter process for flue-gas carbon capture on carbonaceous sorbents: steam-aided vacuum swing adsorption option. Ind. Eng. Chem. Res. 2011;50:9696-703.

[13] Wang L, Liu Z, Li P, Yu J, Rodrigues AE. Experimental and modeling investigation on post-combustion carbon dioxide capture using zeolite 13X-APG by hybrid VTSA process. Chem. Eng. J. 2012;197:151-61.

[14] Choi S, Drese JH, Jones CW. Adsorbent Materials for Carbon Dioxide Capture from Large Anthropogenic Point Sources. ChemSusChem 2009;2:796-854.

[15] Sjostrom S, Krutka H. Evaluation of solid sorbents as a retrofit technology for CO_2 capture. Fuel 2010;89:1298-306.

[16] Lin L-C, Berger AH, Martin RL, Kim J, Swisher JA, Jariwala K, Rycroft CH, Bhown AS, Deem MW, Haranczyk M, Smit B. In silico screening of carbon-capture materials. Nat Mater 2012;11:633-41.

[17] Hedin N, Andersson L, Bergström L, Yan J. Adsorbents for the post-combustion capture of CO2 using rapid temperature swing or vacuum swing adsorption. Appl. Energ. 2013;104:418-33.

[18] Plaza MG, García S, Rubiera F, Pis JJ, Pevida C. Post-combustion CO_2 capture with a commercial activated carbon: Comparison of different regeneration strategies. Chem. Eng. J. 2010;163:41-7.

[19] Plaza MG, García S, Rubiera F, Pis JJ, Pevida C. Evaluation of ammonia modified and conventionally activated biomass based carbons as CO_2 adsorbents in postcombustion conditions. Sep. Purif. Technol. 2011;80:96-104.

[20] Golden TC, Sircar S. Activated carbon adsorbent for PSA driers. Carbon 1990;28:683-90.

[21] Caplow M. Kinetics of carbamate formation and breakdown. J. Am. Chem. Soc. 1968;90:6795-803.

[22] Drage TC, Arenillas A, Smith KM, Pevida C, Piippo S, Snape CE. Preparation of carbon dioxide adsorbents from the chemical activation of urea-formaldehyde and melamine-formaldehyde resins. Fuel 2007;86:22-31.

[23] Pevida C, Plaza MG, Arias B, Fermoso J, Rubiera F, Pis JJ. Surface modification of activated carbons for CO_2 capture. Appl. Surf. Sci. 2008;254:7165-72.

[24] Plaza MG, Rubiera F, Pis JJ, Pevida C. Ammoxidation of carbon materials for CO_2 capture. Appl. Surf. Sci. 2010;256:6843-9.

[25] Plaza MG, Pevida C, Arias B, Fermoso J, Casal MD, Martín CF, Rubiera F, Pis JJ. Development of low-cost biomass-based adsorbents for postcombustion CO_2 capture. Fuel 2009;88:2442-7.

[26] Plaza MG, Pevida C, Martín CF, Fermoso J, Pis JJ, Rubiera F. Developing almond shell-derived activated carbons as CO_2 adsorbents. Sep. Purif. Technol. 2010;71:102-6.

[27] Deitz VR, Carpenter FG, Arnold RG. Interaction of carbon dioxide with carbon adsorbents below 400°C. Carbon 1964;1:245-54.

[28] Sylwester F, Artur PT, Piotr AG, Peter JFH, Piotr K. The influence of carbon surface oxygen groups on Dubinin–Astakhov equation parameters calculated from CO_2 adsorption isotherm. Journal of Physics: Condensed Matter 2010;22:085003.

[29] Liu Y, Wilcox J. Molecular Simulation Studies of CO2 Adsorption by Carbon Model Compounds for Carbon Capture and Sequestration Applications. Environ. Sci. Technol. 2012.

[30] Moreno-Castilla C, Carrasco-Marin F, Mueden A. The creation of acid carbon surfaces by treatment with $(NH_4)_2S_2O_8$. Carbon 1997;35:1619-26.

[31] Jagiello J, Bandosz TJ, Schwarz JA. Application of inverse gas chromatography at infinite dilution to study the effects of oxidation of activated carbons. Carbon 1992;30:63-9.

[32] Saha B, Tai MH, Streat M. Study of activated carbon after oxidation and subsequent treatment. Trans IChemE 2001;79:211-7.

[33] Nelson MR, Borkman RF. Ab Initio calculations on CO_2 binding to carbonyl groups. J. Phys. Chem. A 1998;102:7860-3.

[34] Bell PW, Thote AJ, Park Y, Gupta RB, Roberts CB. Strong Lewis Acid−Lewis Base interactions between supercritical carbon dioxide and carboxylic acids: effects on self-association. Ind. Eng. Chem. Res. 2003;42:6280-9.

[35] Dawson R, Adams DJ, Cooper AI. Chemical tuning of CO2 sorption in robust nanoporous organic polymers. Chemical Science 2011;2:1173-7.

[36] Figueiredo JL, Pereira MFR, Freitas MMA, Órfão JJM. Modification of the surface chemistry of activated carbons. Carbon 1999;37:1379-89.

[37] Bansal RC, Goyal M. Activated carbon adsorption. Boca Raton, FL: CRC Press; 2005.

[38] Tennison SR. Phenolic-resin-derived activated carbons. Applied Catalysis A: General 1998;173:289-311.

[39] Donnet JB. The chemical reactivity of carbons. Carbon 1968;6:161-76.

[40] King A. Studies in chemisorption on charcoal. Part IX. The influence of temperature of activation on the sorption of acids and bases. Journal of the Chemical Society 1937:1489-91.

[41] Brunauer S, Emmett PH, Teller E. Adsorption of gases in multimolecular layers. J. Am. Chem. Soc. 1938;60:309-19.

[42] Noh JS, Schwarz JA. Estimation of the point of zero charge of simple oxides by mass titration. J. Colloid Interface Sci. 1989;130:157-64.

[43] Plaza MG, Pevida C, Arias B, Fermoso J, Arenillas A, Rubiera F, Pis JJ. Application of thermogravimetric analysis to the evaluation of aminated solid sorbents for CO_2 capture. J. Therm. Anal. Calorim. 2008;92:601-6.

[44] Liu Y, Wilcox J. Effects of Surface Heterogeneity on the Adsorption of CO2 in Microporous Carbons. Environ. Sci. Technol. 2012;46:1940-7.

[45] Matsumura Y. Production of acidified active carbon by wet oxidation and its carbon structure. Journal of Applied Chemistry and Biotechnology 1975;25:39-56.

[46] Beck NV, Meech SE, Norman PR, Pears LA. Characterisation of surface oxides on carbon and their influence on dynamic adsorption. Carbon 2002;40:531-40.

[47] Moreno-Castilla C, Ferro-Garcia MA, Joly JP, Bautista-Toledo I, Carrasco-Marin F, Rivera-Utrilla J. Activated carbon surface modifications by nitric acid, hydrogen peroxide, and ammonium peroxydisulfate treatments. Langmuir 1995;11:4386-92.

[48] Plaza MG, Pevida C, Arenillas A, Rubiera F, Pis JJ. CO_2 capture by adsorption with nitrogen enriched carbons. Fuel 2007;86:2204-12.

[49] Pevida C, Snape CE, Drage TC. Templated polymeric materials as adsorbents for the postcombustion capture of CO2. Energ. Procedia 2009;1:869-74.

[50] Martín CF, Plaza MG, Pis JJ, Rubiera F, Pevida C, Centeno TA. On the limits of CO_2 capture capacity of carbons. Sep. Purif. Technol. 2010;74:225-9.

[51] Carson JK, Marsh KN, Mather AE. Enthalpy of solution of carbon dioxide in (water + monoethanolamine, or diethanolamine, or N-methyldiethanolamine) and (water + monoethanolamine + N-methyldiethanolamine) at T= 298.15 K. J. Chem. Thermodyn. 2000;32:1285-96.

[52] Kim I, Svendsen HF. Heat of absorption of carbon dioxide (CO_2) in monoethanolamine (MEA) and 2-(aminoethyl)ethanolamine (AEEA) solutions. Ind. Eng. Chem. Res. 2007;46:5803-9.

[53] Lopez-Ramon MV, Stoeckli F, Moreno-Castilla C, Carrasco-Marin F. On the characterization of acidic and basic surface sites on carbons by various techniques. Carbon 1999;37:1215-21.

[54] Haydar S, Moreno-Castilla C, Ferro-García MA, Carrasco-Marín F, Rivera-Utrilla J, Perrard A, Joly JP. Regularities in the temperature-programmed desorption spectra of CO_2 and CO from activated carbons. Carbon 2000;38:1297-308.

[55] Tremblay G, Vastola FJ, Walker PL. Thermal desorption analysis of oxygen surface complexes on carbon. Carbon 1978;16:35-9.

[56] Bandosz TJ, Ania CO. Surface chemistry of activated carbons and its characterization. In: Bandosz TJ, editors. Activated carbon surfaces in environmental remediation, Amsterdam: Elsevier Ltd.; 2006.

[57] Otake Y, Jenkins RG. Characterization of oxygen-containing surface complexes created on a microporous carbon by air and nitric acid treatment. Carbon 1993;31:109-21.

[58] Voll M, Boehm HP. Basische Oberflächenoxide auf Kohlenstoff—IV. Chemische Reaktionen zur Identifizierung der Oberflächengruppen. Carbon 1971;9:481-8.

[59] Proctor A, Sherwood PMA. X-Ray photoelectron spectroscopic studies of carbon-fiber surfaces .3. Industrially treated fibers and the effect of heat and exposure to oxygen. Surface and Interface Analysis 1982;4:212-9.

[60] Desimoni E, Casella GI, Morone A, Salvi AM. XPS determination of oxygen-containing functional-groups on carbon-fiber surfaces and the cleaning of these surfaces. Surface and Interface Analysis 1990;15:627-34.

[61] Desimoni E, Casella GI, Salvi AM. XPS/XAES study of carbon-fibers during thermal annealing under UHV Conditions. Carbon 1992;30:521-6.

[62] Darmstadt H, Roy C, Kaliaguine S. ESCA characterization of commercial carbon-blacks and of carbon-blacks from vacuum pyrolysis of used tires. Carbon 1994;32:1399-406.

[63] Estrade-Szwarckopf H. XPS photoemission in carbonaceous materials: A "defect" peak beside the graphitic asymmetric peak. Carbon 2004;42:1713-21.

[64] Puziy AM, Poddubnaya OI, Socha RP, Gurgul J, Wisniewski M. XPS and NMR studies of phosphoric acid activated carbons. Carbon 2008;46:2113-23.

List of Tables

List of Figures